

## Simulation and analysis of a fuel supply system with vent control system for ammonia fueled ships

Seong-kyu Jeong<sup>1</sup> · You-Taek Kim<sup>2</sup> · Jun-Seong Kim<sup>†</sup>

(Received October 3, 2024 ; Revised October 15, 2024 ; Accepted October 21, 2024)

**Abstract:** Process system modeling and dynamic simulation of the ammonia fuel supply system for a 320,000 dwt Very large crude carrier (VLCC) were conducted in this study. Focusing on the International maritime organization (IMO) 2050 decarbonization goals and the potential of ammonia as a carbon-free fuel, key process parameters and engine performance for the ammonia fuel system design were analyzed. The process design was based on WinGD's X72DF-A-1.0 ammonia dual-fuel engine, evaluating fuel consumption, system efficiency, and vent control methods. The system was designed with a fuel supply mechanism utilizing both low-pressure and high-pressure pumps from the fuel tank, with ammonia fuel consumption at maximum output estimated at 9,384 kg/h. Additionally, instead of absorbing ammonia from operational ventilation into seawater, an absorption-based ammonia vent control system was proposed to meet relevant regulations (below 25 ppm), resulting in the production of less than 1 ton of wastewater for each set of vent operations. Through dynamic simulation using Aspen HYSYS, the operational stability of the system was verified, and optimal operating conditions for fuel change and vent control were identified. The study demonstrates that the ammonia fueled ship system meets IMO regulations and has potential as a viable alternative fuel.

**Keywords:** Decarbonization, Ammonia fueled ship, Ammonia fuel supply system, Vent control system, Dynamic simulation

### Nomenclature

bar(g)	bar gauge
G	Gibbs energy of a component
$\gamma$	Activity coefficient of component
Kc	Proportional gain of control
Ti	Integral time of control

MDO	Marine diesel oil
NRTL	Non-random two liquid
SGC	Specific gas consumption
SPC	Specific pilot oil consumption
UA	Overall heat transfer coefficient
VLE	Vapor-liquid equilibrium
VLCC	Very large crude carrier
VLEL	Vapor-liquid-liquid equilibrium

### Abbreviation

BSGC	Brake specific gas consumption
BSPC	Brake specific pilot oil consumption
HFO	Heavy fuel oil
IMO	International maritime organization
LHV	Lower heating value
LIC	Level indicator controller
MCR	Maximum continuous rating
MEPC	Maritime environment protection committee

## 1. Introduction

IMO has set a decarbonization goal to reduce greenhouse gas emissions from the shipping sector by at least 50% by 2050, and in 2023, the Marine Environment Protection Committee (MEPC) presented targets to reduce carbon intensity by 40% by 2030 compared to 2008 levels and to achieve carbon neutrality for ships by 2050 [1][2]. These targets have accelerated global research into renewable energy and zero-carbon alternative fuels for ships [3].

<sup>†</sup> Corresponding Author (ORCID: <https://orcid.org/0000-0001-6151-2649>): Assistant professor, Division of Marine System Engineering, Korea Maritime & Ocean University, 727, Taejong-ro, Yeongdo-gu, Busan 49112, Korea, E-mail: [jskim87@kmou.ac.kr](mailto:jskim87@kmou.ac.kr), Tel: +82-51-410-4266

1 Researcher, Advanced propulsion system R&D team, Hanwha Ocean, E-mail: [skjeong@hanwha.com](mailto:skjeong@hanwha.com), Tel: +82-2-2129-7235

2 Professor, Division of Marine System Engineering, Korea Maritime & Ocean University, E-mail: [kimyt@kmou.ac.kr](mailto:kimyt@kmou.ac.kr), Tel: +82-51-410-4258

This is an Open Access article distributed under the terms of the Creative Commons Attribution Non-Commercial License (<http://creativecommons.org/licenses/by-nc/3.0>), which permits unrestricted non-commercial use, distribution, and reproduction in any medium, provided the original work is properly cited.

According to international regulations established by the IMO, reducing carbon emissions from ships can be achieved through the exclusive use of alternative fuels or their blending with conventional fuels [4].

Ammonia does not emit carbon dioxide during combustion, and one of its primary components, nitrogen, is abundantly available in the atmosphere, making ammonia relatively easy to produce [5]. Liquid ammonia has a density approximately 850 times that of its gaseous state at atmospheric pressure and has a boiling point about  $-33.4^{\circ}\text{C}$  at atmospheric pressure [6]. Therefore, its physical properties must be carefully considered when designing fuel storage tanks, fuel supply systems, and other components, like other liquefied gas fuels.

The ammonia engines currently being developed for large ships include MAN-ES's ME-LGIA (Liquid Gas Injection Ammonia) and WinGD's X-DF-A (Dual Fuel Ammonia). Both models are undergoing land-based testing based on the diesel cycle, and the first engines are expected to be delivered to shipyards in late 2024 or early 2025 [7]. According to information released by the engine manufacturers, both engines are dual-fuel engines capable of operating on ammonia as well as diesel fuel, and the injection rate of pilot oil required for ignition in gas mode is expected to be more than 5% [8].

Consequently, the development of ammonia fueled ships is currently underway, and research into fuel supply systems for these developing ammonia engines, as well as into vent control system that can meet environmental regulations when toxic ammonia gas is emitted into the atmosphere, is actively progressing. Although engine makers and equipment manufacturers are developing related systems, there is a lack of clarity in the treatment methods and capacity estimation criteria, necessitating further study in this area. Due to the toxicity of ammonia fuel, special design considerations different from conventional marine fuel systems are required.

In this study, dynamic simulations and process analyses of the ammonia fuel supply system and vent control system applicable to a 320,000 dwt VLCC are performed using data from the X-DF-A engine by WinGD, which is the only manufacturer that has disclosed its engine data. The main objective of this study is to simulate the process of the ammonia fuel supply system and propose a method to safely handle ammonia gas through the vent control system. Based on this analysis, the aim is to enhance the practical applicability of ammonia fueled ships and propose safer and more efficient systems.

## 2. Process Simulation

### 2.1 Selection of Reference Engine

For the modeling of the ammonia fuel supply system, the reference engine was selected as the main engine applied to a 320,000 dwt VLCC, based on engine specifications provided by MAN-ES for a VLCC. The selection was made considering a service speed of 15 knots, an MCR of 23,500 kW, and a propeller speed of 73.4 rpm [9].

The applicable ammonia engine for the 320,000 dwt VLCC is the WinGD X72DF-A-1.0, with an 8-cylinder configuration designed for 23,500 kW output at 73.4 rpm. The fuel consumption rate based on engine output is shown in Table 1.

**Table 1:** 8X72DF-A-1.0 Engine data

Load	Power	Speed	BSGC	BSPC
%	kW	rpm	g/kWh	g/kWh
110	25850	73.4	-	-
105	24675	73.4	-	-
100	23500	73.4	363	8.5
95	22325	73.4	354.9	8.9
90	21150	73.4	346.4	9.4
85	19975	73.4	340.7	9.9
80	18800	73.4	337.4	10.6
75	17625	73.4	334.9	11.2
70	16450	73.4	329.4	12.1
65	15275	73.4	323.8	13
60	14100	73.4	324.2	14.1
55	12925	73.4	324.7	15.4
50	11750	73.4	324.7	16.9
45	10575	73.4	323.3	18.8
40	9400	73.4	322.1	21.2
35	8225	73.4	318.3	24.1
30	7050	73.4	317.5	28.2
25	5875	73.4	310.5	33.8

When operating at maximum power, the engine's specific gas consumption (SGC) is 8,531 kg/h, and the specific pilot oil consumption (SPC) is 200 kg/h. However, since the engine needs to operate at up to 110% of its power output during sea trials, the fuel supply system flow rate was set at 9,384 kg/h.

Considering the lower heating value (LHV) of ammonia as 18,600 kJ/kg and that of pilot oil as 42,700 kJ/kg, the thermal efficiency at maximum power output is calculated to be 50.6%. This indicates that there is no significant efficiency difference

compared to conventional gas engines when using ammonia as a fuel.

## 2.2 System Configuration

The system configuration includes the installation of an IMO Type-C independent tank on the VLCC, with a low-pressure pump inside the fuel tank and a high-pressure pump located outside the tank to pressurize ammonia to 85 bar(g). In the process system design, ammonia fuel is pressurized by the low-pressure pump inside the fuel tank and sent to the suction side of the high-pressure pump in the fuel preparation room. The high-pressure pump then further pressurizes the ammonia fuel to 85 bar(g), meeting the fuel supply conditions of the X72DF-A-1.0 engine before delivering it to the engine. The temperature of the ammonia fuel inside the tank corresponds to its saturation temperature at tank pressure, which is  $-33.4^{\circ}\text{C}$ . When pressurized by the low-pressure pump, a temperature rise is observed due to pump efficiency, resulting in a temperature of  $-31.5^{\circ}\text{C}$  at the inlet of the heat exchanger, which was used as the basis for calculating the heat exchanger capacity.

As ammonia is toxic and harmful to human health and causes air pollution when released into the atmosphere, strict regulations are applied to its handling, and the IMO is expected to prohibit the direct atmospheric release of ammonia. In this study, the system is designed to process ammonia vent gas to a concentration of 25 ppm or less, a standard based on the American Bureau of Shipping (ABS) regulations, which serves as a reference for vent control system in ammonia fueled ships [10]. In domestic on-shore ammonia gas refueling stations, large absorption-type water tanks are used to prevent atmospheric release of ammonia gas. For ships, the simplest approach would be to absorb ammonia in seawater and discharge it into the ocean. However, since there are ongoing discussions to regulate not only atmospheric but also marine discharge of ammonia from ships, this study designs a system utilizing an absorption-based ammonia vent control system, with the resulting wastewater stored onboard.

Aspen HYSYS v10 was utilized to model and simulate the ammonia fuel supply system and vent control system [11]. This tool is widely applied in thermal, fluid, and chemical process modeling, ensuring reliability in the results of the simulations [12].

## 2.3 Equation of State

Process simulation software typically models systems based on equations of state, which describe the conditions of a substance. Although the ideal gas law can be used as a fundamental equation of state, it assumes no intermolecular interactions and neglects

molecular volume, leading to discrepancies when compared to the behavior of real substances.

The Refprop program suggests calculating the equation of state for ammonia based on Helmholtz energy. Since the ammonia used in this study is anhydrous with minimal impurities, common equations of state provided by Aspen HYSYS, such as Peng-Robinson, MBWR, and NRTL, can be appropriately applied for process system simulation [13].

However, in the case of the absorption-based ammonia vent control system addressed in this study, it is necessary to account for the absorption reaction. According to previous research, the Non-Random Two-Liquid (NRTL) equation of state is suitable for modeling the vapor-liquid equilibrium of the ammonia-water system. Therefore, the NRTL equation of state was used for process simulation in this study [14].

The NRTL equation of state in HYSYS software is an extended model of the Wilson equation, utilizing statistical mechanics and liquid cell theory to represent liquid structures. It is capable of describing vapor-liquid equilibrium (VLE), liquid-liquid equilibrium (LLE), and vapor-liquid-liquid equilibrium (VLLE) states. The fundamental form of the NRTL equation is presented in Equation (1).

$$\ln \gamma_i = \frac{\sum_{j=1}^n (\tau_{ji} x_j G_{ji})}{\sum_{k=1}^n (x_k G_{kj})} + \sum_{j=1}^n \left( \frac{x_j G_{ij}}{\sum_{k=1}^n (x_k G_{kj})} \right) \left( \tau_{ij} - \frac{\sum_{m=1}^n (\tau_{im} x_m G_{mj})}{\sum_{k=1}^n (x_k G_{kj})} \right) \quad (1)$$

Where  $\gamma_i$  represents activity coefficient of component  $i$ ,  $\tau_{ji}$  represents interaction parameter for component between components  $j$  and  $i$ ,  $x_j$  represents Mole fraction of component  $j$ ,  $G_{ji}$  represents Gibbs energy of component  $j$  with respect to component  $i$ .

## 2.4. System Modeling

The fuel supply system was configured and specifications for each component were determined under the condition that the X72DF-A-1.0 engine is applied as the main engine for a 320,000 dwt VLCC. The system consists of an IMO Type-A independent tank installed on the VLCC, with a low-pressure pump located inside the fuel tank and a high-pressure pump outside the tank to pressurize ammonia to 85 bar(g).

Since all evaporative gas generated during operation in the ammonia fuel tank must be processed, the low-pressure pump is designed so that its discharge pressure is at least the minimum suction pressure of the high-pressure pump.

This design ensures that no evaporative gas is generated, even when the system reaches its design temperature. To prevent icing during abnormal operation, glycol water was selected as the heating medium for the fuel heater. The system was designed to supply

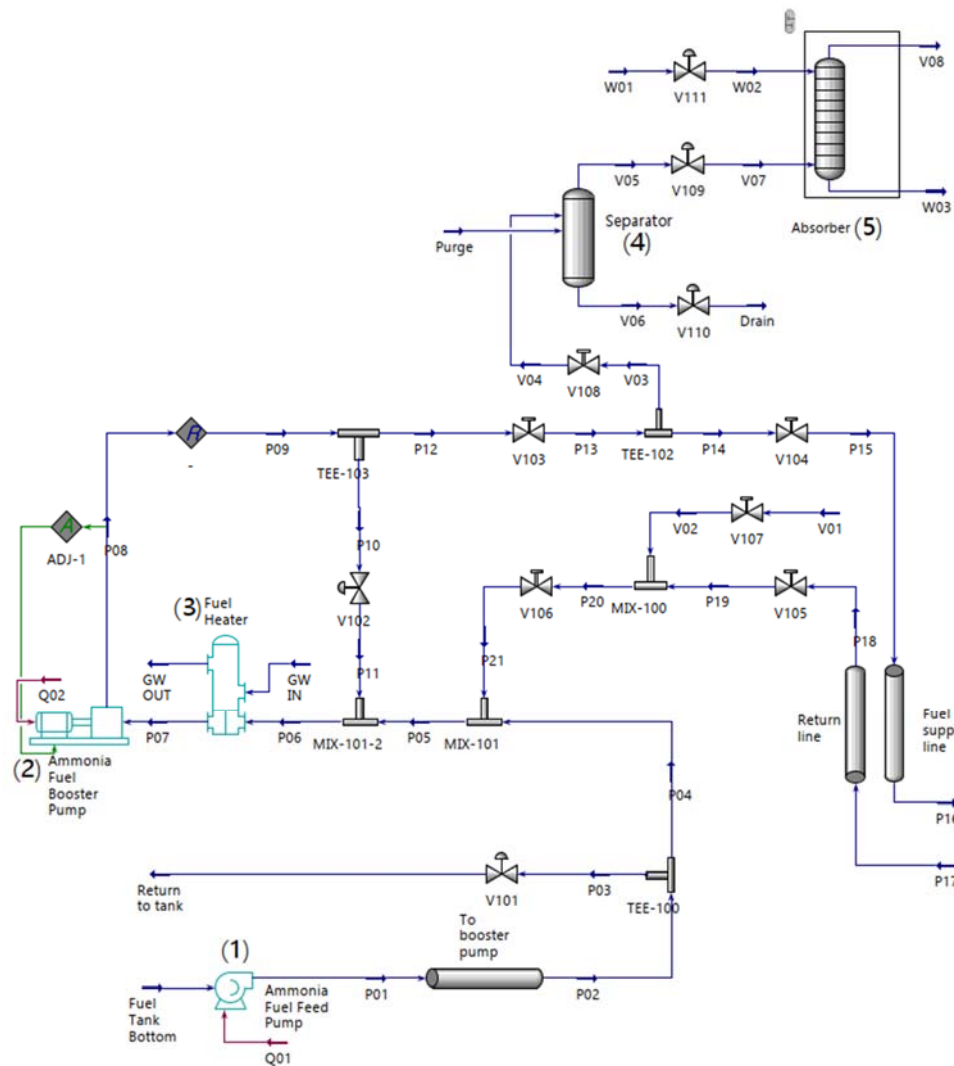


Figure 1: HYSYS Steady simulation for ammonia fuel supply system

heat through the heat exchange between glycol water and steam.

Figure 1 shows the static simulation of the system. The low-pressure pump (1) inside the fuel tank (Ammonia fuel feed pump) pressurizes the ammonia fuel and sends it to the suction side of the high-pressure pump (2) (Ammonia fuel booster pump) located in the fuel preparation room. The high-pressure pump further pressurizes the ammonia fuel to 85 bar(g), which meets the fuel supply conditions of the X72DF-A-1.0 engine, and then supplies it to the engine. The temperature of the ammonia fuel inside the tank is  $-33.4^{\circ}\text{C}$ , which is the saturation temperature at the tank pressure. A temperature increase is observed during pressurization by the low-pressure pump, attributed to pump efficiency. The temperature at the inlet of the heat exchanger (3) (Fuel heater) is  $-31.5^{\circ}\text{C}$  when there is no external heat ingress, which was used as the basis for calculating the capacity of the heat exchanger.

The heat exchanger (3), located upstream of the high-pressure pump (2), raises the temperature of the ammonia fuel to the required engine supply temperature. It also ensures that the fuel temperature remains above the pour point of any sealing oil present within the fuel supply system before the ammonia fuel is delivered to the high-pressure pump. Given the relatively low operating pressure of 25 bar(g), heat exchangers commonly used in ships, such as the shell-and-tube type or shell-and-plate type, can be applied.

The high-pressure pump (2) was selected to have a suction pressure of 25 bar(g) and a discharge pressure that exceeds the engine's requirement of 85 bar(g), with the pump head of the modeled pump being 1077 meters.

According to classification society regulations, it is anticipated that ammonia gas generated during operation shall be treated to a concentration of 25 ppm or less before atmospheric release.

While the simplest approach on a ship would be to absorb the ammonia in seawater and discharge it into the ocean, there are ongoing discussions to prohibit both atmospheric and marine discharge of ammonia. Therefore, this study employs an absorption-based ammonia vent control system comprising a gas-liquid separator (4) and an absorber (5), with the generated wastewater stored onboard. The vent gas generated during operation consists of nitrogen and ammonia, and since only ammonia, which is restricted from atmospheric release, needs to be absorbed, water was used as the absorbent. The nitrogen can be safely released into the atmosphere.

The key parameters of pressure, temperature, flow rate, power consumption, and heat duty for each component, calculated based on the process system modeling, are summarized in **Table 2**.

**Table 2:** Process design result for ammonia fuel supply system

	Fuel feed pump	No.2 Heat exchanger	Booster pump
Inlet Pressure	0.17 bar(g)	25.39 bar(g)	25.29 bar(g)
Outlet Pressure	25.57 bar(g)	25.29 bar(g)	86.14 bar(g)
Inlet Temperature	-33.45 °C	-31.51 °C	40.0 °C
Outlet Temperature	-31.51 °C	40.0 °C	43.11 °C
Power Consumption	25.08 kW	-	44.39 kW
Flow rate (Ammonia)	9853 kg/h	9853 kg/h	9853 kg/h
Flow rate (Glycol water)	-	223.6 m <sup>3</sup> /h	-
Heat Duty	-	956.2 kW	-
Overall UA	-	45,540 W/C	-

### 3. System Operation Simulation

#### 3.1. Dynamic Simulation

Using the process simulation modeling, a dynamic simulation was performed to analyze the operation of the fuel supply system. **Figure 2** shows the dynamic simulation of the system. The operation of each pump was controlled by pressure regulation within the recirculation line, while the vent control system was managed by controlling the vapor pressure and liquid level of the gas-liquid separator.

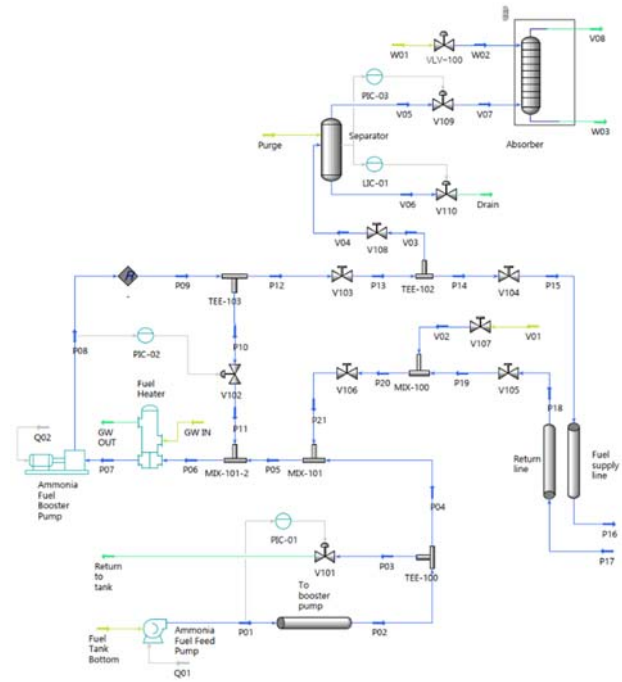


**Figure 2:** HYSYS Dynamic simulation for ammonia fuel supply system

The fuel supply line was designed with 40A piping to account for pressure drops when the engine operates at maximum output, while the fuel return line uses 25A piping, considering nitrogen purging operations. Assuming a piping length of 100 m, the total volume was calculated to be 175 liters, with the fuel supply line accounting for 126 liters and the fuel return line for 49 liters.

To establish the process conditions for the vent control system, an analysis was deemed necessary for the scenario involving gas discharge from the fuel line after an emergency shutdown, as it has a higher flow rate than during fuel switching.

In the event of an emergency shutdown, the discharge of gas from the fuel line involves stopping both the high-pressure and low-pressure pumps, closing the supply valve (V103) and return valve (V106) in the valve train, and purging the fuel line and engine gas fuel system with nitrogen. During this process, purge gas is supplied through V107, and ammonia fuel is sent to the gas-liquid separator via V108. P16 and P17 are directly connected via the engine's fuel gas manifold, allowing the fuel line, including the fuel gas manifold, to be purged with nitrogen during the purge operation.

Operating the gas-liquid separator at a pressure higher than the saturation pressure of ammonia at its operating temperature can reduce the flow rate discharged to the absorber. However, since nitrogen is present in the fluid supplied to the gas-liquid separator

during the nitrogen purge of the fuel system, raising the operating pressure has limited effect on reducing gas discharge. Additionally, there are constraints on increasing the nitrogen supply pressure, and with the use of 30 bar(g) nitrogen applied on ammonia carriers, the operating pressure was set at 22 bar(g), which is higher than the saturation pressure of ammonia at the maximum operating temperature of 50°C (19.3 bar(g)), to minimize the amount of evaporative gas.

The nitrogen-ammonia mixed gas sent to the gas-liquid separator is discharged to the absorber through V109, while the liquid is either stored in the gas-liquid separator or sent back to the fuel tank via V110 when the liquid level in separator is high.

A nitrogen flow rate of 250 kg/h was supplied through V107 for the dynamic analysis, and the results showed that nitrogen replaced the ammonia in the fuel piping, causing a mixture of ammonia and nitrogen gas to be discharged from the vapor phase of the gas-liquid separator.

Four controllers were employed in the dynamic simulation, all using PI (Proportional, Integral) control. The valve positions were assumed to be at 50% under design conditions, and the actuator stroke speed was set at 12.5% per second [15]. The control parameters, Kc (proportional gain) and Ti (integral time), were tuned using the Aspen HYSYS tuning functionality and are presented in Table 3.

**Table 3:** Process variables and control parameters

Tag	Process Variable	Kc	Ti
PIC-01	Feed pump discharge pressure	2.21	0.733
PIC-02	Booster pump discharge pressure	14.7	0.700
PIC-03	Separator pressure	13.2	0.733
LIC-01	Separator level	12.1	2.2

The completion of ammonia discharge from the fuel line was assessed based on when the vapor fraction at V04 reached 1. At this point, a review of the dynamic simulation data log of the flow rate at V05, which discharges from the gas-liquid separator to the absorber, indicated that the liquid ammonia in the piping was replaced by nitrogen within 200 seconds of the start of the nitrogen purge, as shown in Figure 3. When operating the gas-liquid separator at 22 bar(g), the discharged gas flow rate gradually increased to a maximum of 296 kg/h by 240 seconds, after which the mass flow rate of the discharged gas gradually decreased while maintaining a vapor fraction of 1 in the piping.

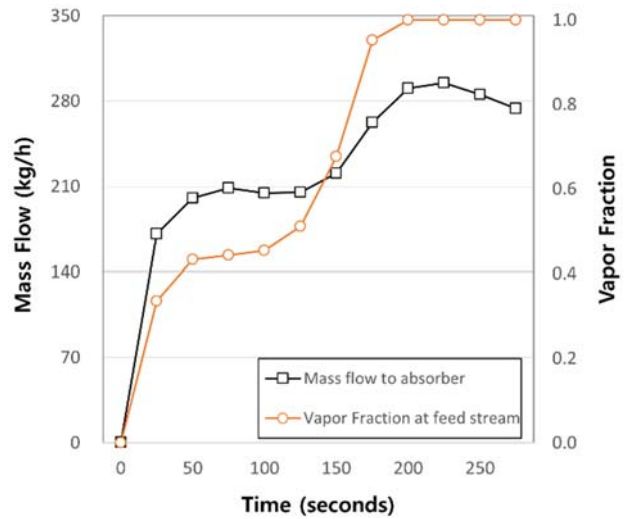


**Figure 3:** Vapor fraction of vent gas

As shown in Figure 4, the composition of the vent gas at the start of the operation was 0.8 ammonia and 0.2 nitrogen, but as the purge operation of the fuel piping progressed, the nitrogen composition gradually increased. During the initial phase of ammonia discharge from the fuel line, a mixture of liquid ammonia and nitrogen was sent through the gas-liquid separator to the absorber. As the liquid ammonia in the piping was replaced by nitrogen, the mass flow rate increased, reaching a maximum of 296 kg/h after the vapor fraction reached 1, and the gas composition was 0.6 ammonia and 0.4 nitrogen.

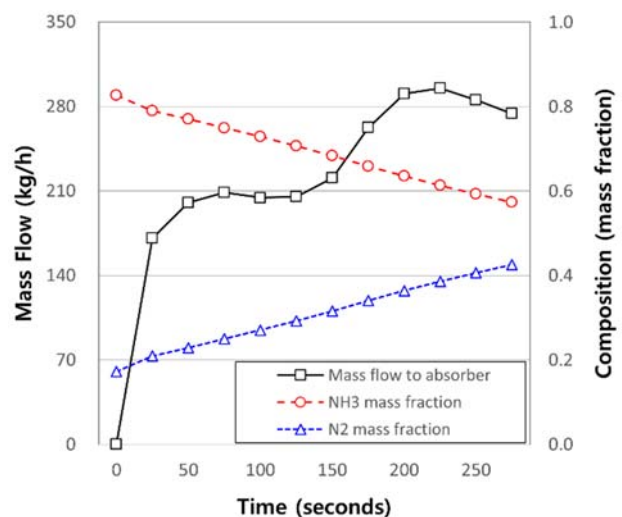


**Figure 4:** Gas composition in vent gas

### 3.2. Vent Control System

The vent control system consists of a gas-liquid separator, an absorber, and a bilge tank. These components must be installed within



an explosion-proof area in accordance with regulations for the application of low-flashpoint fuels on ships.

Using the dynamic analysis results, a process simulation was conducted for the absorber, which is the main component of the vent control system. The flow rate of the fresh water used as the absorbent was set to ensure that the ammonia concentration at the gas outlet of the absorber is kept below 10 ppm. The absorber was modeled with 10 theoretical stages to calculate the required flow rate of the absorbent using Aspen HYSYS.

To optimize the flow rate of the absorbent supplied via W02, the process simulation was conducted based on the maximum flow rate of 300 kg/h of the ammonia-nitrogen mixed gas supplied via V07. The flow rate of the absorbent, the composition of the vent gas, and the mass flow rate and composition of the resulting bilge water were assessed.

Under these conditions, the results of the simulation, as shown in **Figure 5**, indicate that the required absorbent flow rate is 5,251 kg/h, the flow rate of the vent gas is 125 kg/h, and the flow rate of the ammonia-containing bilge water is 5,426 kg/h with an ammonia concentration of 3.3%. According to the dynamic analysis of the system, ammonia is fully purged from the piping within approximately 200 seconds. Therefore, in this study, a single purge operation was assumed to last for 5 minutes. As a result, it was found that 437.6 kg of fresh water is required to perform the purge operation for 5 minutes to replace the ammonia in the fuel piping with nitrogen, and the amount of ammonia bilge generated is 452.2 kg.

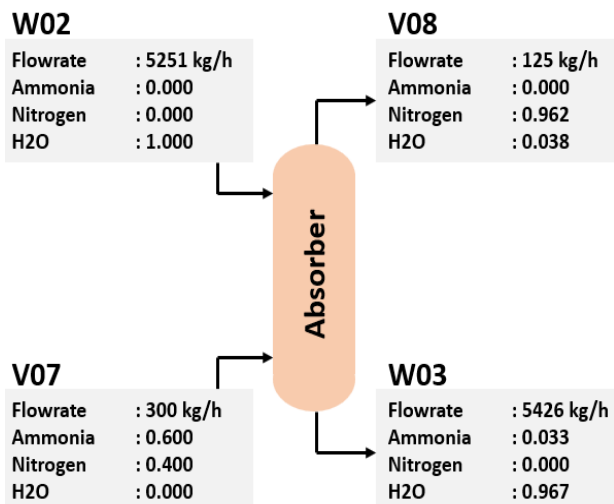


**Figure 5:** In-Out Stream Conditions of the Absorber

The absorption-based vent control system requires storage space for both the supply of the absorbent and the storage of the generated bilge water. Based on 10 purge operations, the required freshwater

volume is 4,376 kg, and the amount of ammonia bilge generated is 4,522 kg. Therefore, an additional 4.4 tons of fresh water must be produced for 10 purge operations, and a bilge tank with a capacity of over 5 m<sup>3</sup> should be installed within the hazardous area.

## 4. Conclusion

In this study, a process simulation for a 320,000 dwt VLCC was performed to establish the process system and operational conditions for an ammonia fueled ship, with the aim of conducting dynamic simulations.

Based on the review of published classification society regulations and engine manufacturer data, the process system modeling conditions were set to include a fuel supply pressure of 85 bar(g) and a purge vent limit of 25 ppm for ammonia gas. The HYSYS process simulation was carried out using the NRTL equation of state.

The dynamic simulation and analysis results showed that within 200 seconds of initiating nitrogen purging, the liquid ammonia inside the piping was replaced with nitrogen, reaching a vapor fraction of 1. When the pressure of the gas-liquid separator was controlled at 22 bar(g), the flow rate of the discharged gas increased gradually until reaching a maximum of 296 kg/h at 240 seconds, after which the flow rate decreased while maintaining a vapor fraction of 1 in the piping. Initially, the composition of the vent gas was 0.8 ammonia and 0.2 nitrogen, and as the purge operation of the fuel supply line progressed, the nitrogen composition increased.

When the absorption-based vent control system was applied, the flow rate of the freshwater absorbent was 5,251 kg/h. Under actual operating conditions, the consumption of fresh water for a single purge operation during fuel switching was 437.6 kg, and the resulting ammonia bilge produced was 452.2 kg, discharged as an aqueous solution containing 3.3% ammonia.

The use of ammonia fuel in ships showed many technical similarities to conventional low-flashpoint fuel systems. However, considering the overall increase in equipment capacity due to the lower heating value of ammonia and the need for additional equipment for vent control system and ammonia bilge handling, it is necessary to consider these factors when applying ammonia fuel for actual ship propulsion systems.

## Author Contributions

Conceptualization, S. K. Jeong and J. S. Kim; Methodology, S. K. Jeong and J. S. Kim; Software, S. K. Jeong; Formal

Analysis, S. K. Jeong; Investigation, S. K. Jeong and J. S. Kim; Resources, Seong-kyu Jeong; Data Curation, S. K. Jeong; Writing-Original Draft Preparation, S. K. Jeong; Writing-Review & Editing, Y. T. Kim and J. S. Kim; Visualization, S. K. Jeong; Supervision, Y. T. Kim and J. S. Kim.

## References

- [1] IMO, Initial IMO Strategy on Reduction of GHG Emissions from Ships, Resolution MEPC.304(72) (Adopted on 13 April 2018), MEPC 72/17/Add.1, 1–10, 2018.
- [2] K. Bayramoğlu, “The effects of alternative fuels, cruising duration and variable generators combination on exhaust emissions, energy efficiency existing ship index (EEXI) and carbon intensity rating (CII),” *Ocean Engineering*, vol. 302, 2024.
- [3] H. Jang, M. P. Mujeeb-Ahmed, H. Wang, C. Park, I. Hwang, B. Jeong, P. Zhou, and R. Mickeviciene, “Regulatory gap analysis for risk assessment of ammonia-fuelled ships,” *Ocean Engineering*, vol. 287, Part 2, 2023.
- [4] H. Xing, C. Stuart, S. Spence, and H. Chen, “Alternative fuel options for low carbon maritime transportation: Pathways to 2050,” *Journal of Cleaner Production*, vol. 297, 2021.
- [5] S. Jeong, J. Kim, and Y. -T. Kim, “Optimization study of BOG re-liquefaction process for ammonia fueled ship,” *Journal of Advanced Marine Engineering and Technology*, vol. 48, no. 4, pp. 167-176, 2024.
- [6] S. CROLIUS, D. PUGH, S. MORRIS and A. VALERAMEDINA, “Safety Aspects,” in *Techno-Economic Challenges of Green Ammonia as an Energy Vector*, Elsevier Inc., pp. 221-257, 2021.
- [7] MAN Energy Solutions, *Alternative fuels for your two-stroke powered vessel, Ammonia, methanol and methane in focus*, 2024.
- [8] WinGD, *GTD – General Technical Data for WinGD 2-Stroke Engines*, 2024.
- [9] MAN Diesel & Turbo, “Propulsion of VLCC,” 2016.
- [10] ABS Requirement for Ammonia Fueled Vessels, 2023.
- [11] Aspen HYSYS v.10 user guide.
- [12] A. Sunny, P. A. Solomon, and K. Aparna, “Syngas production from regasified liquefied natural gas and its simulation using Aspen HYSYS,” *Journal of Natural Gas Science and Engineering*, vol. 30, pp. 176-181, 2016.
- [13] Kh. Mejbri and A. Bellagi, “Modelling of the thermodynamic properties of the water–ammonia mixture by three different approaches,” *International Journal of Refrigeration*, vol. 29, no. 2, 2006.
- [14] M. Wang, T. M. Becker, C. A. Infante Ferreira, “Assessment of vapor–liquid equilibrium models for ionic liquid based working pairs in absorption cycles,” *International Journal of Refrigeration*, vol. 87, pp. 10-25, 2018.
- [15] R. Elyas, “Chapter 15 - Dynamic simulation for process control with Aspen HYSYS,” *Chemical Engineering Process Simulation (Second Edition)*, Elsevier, pp. 309-341, 2023.